Structural investigations of polymer electrolyte poly(propylene oxide)–$LiClO_4$ using diffraction experiments and reverse Monte Carlo simulation

ARTICLE *in* THE JOURNAL OF CHEMICAL PHYSICS · DECEMBER 2004

Impact Factor: 2.95 · DOI: 10.1063/1.1815295 · Source: PubMed

6 AUTHORS, INCLUDING:

Patrik Carlsson
Chalmers University of Technology
21 PUBLICATIONS **127** CITATIONS
SEE PROFILE

Jan Swenson
Chalmers University of Technology
177 PUBLICATIONS **3,992** CITATIONS
SEE PROFILE

William Spencer Howells
Science and Technology Facilities Council
268 PUBLICATIONS **3,408** CITATIONS
SEE PROFILE

Lars Börjesson
Chalmers University of Technology
329 PUBLICATIONS **6,482** CITATIONS
SEE PROFILE

Structural investigations of polymer electrolyte poly(propylene oxide)-$LiClO_4$ using diffraction experiments and reverse Monte Carlo simulation

P. Carlsson, D. Andersson,[a] and J. Swenson
Department of Applied Physics, Chalmers University of Technology, SE-412 96 Göteborg, Sweden

R. L. McGreevy and W. S. Howells
Rutherford Appleton Laboratory, Chilton, Didcot OX11 0QX, United Kingdom

L. Börjesson
Department of Applied Physics, Chalmers University of Technology, SE-412 96 Göteborg, Sweden

(Received 17 June 2004; accepted 21 September 2004)

The structure of an amorphous polymer electrolyte, poly(propylene oxide) (PPO) complexed with $LiClO_4$, has been studied using reverse Monte Carlo (RMC) simulations. The simulations require no force field but are based on experimental data only, in this case from x-ray and neutron diffraction experiments. Excellent agreement between the experimental data and the structures resulting from the RMC simulation is obtained. Samples with ether-oxygen to lithium concentrations (molar ratios) O:Li=16:1 and 5:1 were studied and compared to results of pure PPO from a previous study. We focus on the effects of the solvated salt on the structure of the polymer matrix, the spatial distribution of ions, and the correlations between the anions and the polymer chains. Analyzing the structures produced in the simulations, we find that for a concentration 16:1, the interchain distance is approximately the same as in pure PPO but more well defined. For a concentration 5:1, we find a larger and less well-defined interchain distance compared to the 16:1 concentration. This signifies that at the 16:1 salt concentration, there is enough free volume in the polymer host to accommodate the ions, and that the solvation of salt induces ordering of the polymer matrix. At the higher salt concentration 5:1, the polymer network must expand and become less ordered to host the ions. We also note, in accordance with previous studies, that the solvation of salt changes the conformation of the polymer chain towards more *gauche* states. The simulations furthermore reveal marked correlations between the polymer chains and the anions, which we suggest arise predominantly from an interaction mediated via cations, which can simultaneously coordinate both ether oxygens in the polymer chains and anions. Interanionic distances at 5 Å, which are consistent with two or more anions being coordinated around the same cation, are also observed. On a larger scale, the RMC structure of PPO-$LiClO_4$ 16:1 clearly indicates the presence of salt-rich and salt-depleted domains having a length scale of <20 Å. In view of such a heterogeneous structure of PPO-$LiClO_4$ 16:1, it is plausible that the increased ordering of the polymer matrix is due to rather well-defined structural arrangements within the salt-rich domains, and that the characteristic interchain distance in the salt-rich domains is similar to that of the pure polymer. © *2004 American Institute of Physics.* [DOI: 10.1063/1.1815295]

I. INTRODUCTION

There is currently a worldwide interest in polymer electrolytes, mainly due to applications in new nontoxic and cheap batteries with high energy density. Complexes of a range of different polymers and salts have been prepared and tested since the first discovery that polymer-salt complexes may function as polymer electrolytes.[1] Substantial advances have been made using different cross links, fillers, plasticizers, etc., to improve the mechanical properties and to obtain highly ion-conducting materials. Impressive efforts in characterizing polymer electrolytes have been demonstrated and considerable insight has been gained over the years;[2,3] yet the ion conduction mechanism is not fully understood. A better understanding is important since pure polymer electrolytes with their inherent advantages, still have too low conductivities to be viable in room temperature applications.

The ionic conductivity in electrolytes based on polyethers, such as poly(ethylene oxide) (PEO) and poly(propylene oxide) (PPO), is closely linked to the structural dynamics of the polymer segments,[3–5] and much effort has been devoted to investigate how the segmental dynamics is affected by salt solvation.[6] It can be expected that the interaction between the solvated salt and the polymer segments is reflected in the structure of the electrolyte. Hence, for a better understanding of the ion conduction mechanism it is important to investigate, for instance, how the structure of the polymer network is affected by salt solvation, the coordina-

[a]Electronic mail: dma@fy.chalmers.se

tion of ions to the polymer segments, and the spatial distribution of the solvated salt.

The knowledge about structural properties of polymer electrolytes is, in this perspective, rather limited. The crystalline structures of a range of different poly(ethylene oxide) complexes have been characterized using diffraction methods.[7–14] The conformation of the polymer chain changes from a stretched zig zag in 1:1 complexes, through a helix around the cations in 3:1 and 4:1 complexes, to two interlocking half cylinders enclosing the cations when the O:Li ratio is 6:1,[15] though the relevance of the crystalline structures for the mechanism of ion conduction may be limited since the ion conduction takes place mainly in the amorphous phase.[16]

Structural studies of the amorphous phase are, however, scarce. Molten PEO-LiI has been successfully investigated by combining neutron diffraction[17,18] and molecular dynamics simulations.[19,20] The structures of molten PEO-LiTFSI (Ref. 21) and PEO-$LiClO_4$ (Ref. 22) have also been studied using neutron diffraction. The diffraction studies were performed with isotopic substitution for lithium, and bond lengths and coordination numbers were calculated and compared to *ab initio* or molecular dynamics (MD) simulation results. We have in previous studies investigated an inherently amorphous polymer electrolyte, PPO complexed with $LiClO_4$,[23–26] using neutron scattering. In these studies, structural information was mainly derived by comparing the data with the structure of pure PPO, which was characterized in a detailed study using reverse Monte Carlo (RMC) simulations.[27]

The coordination of ions in polymer electrolytes is complex; different ionic coordinations have been observed, from single cations completely solvated by the ether oxygens of the polymer chains to more complex arrangements involving various polymer-cation-anion interactions.[28–31] The cations generally act as a coordination center of several ether oxygens, either coordinating oxygens within a single chain or those belonging to adjacent chains. When the cations coordinate ether oxygens of different chains, they act as transient cross links, and is a possible cause of the observed slowing down of the polymer segmental motion[4] and the increase in the viscosity and the glass transition temperature T_g (Refs. 32–34) as salt is introduced in PPO systems.

Another sign of the special solvation properties of polyether-salt systems is the indication of structural heterogeneity on microscopic length scales; two different glass transitions have been observed in polyether-salt systems and were attributed to salt-rich and salt-depleted domains.[35,36] For salt concentrations higher than O:Li=10:1 only the salt-rich structure was proposed to be present in the PPO-$LiClO_4$ system. This is of course of high interest, since a heterogeneous distribution of the salt in the polymer matrix must have implications on the mechanism of ion conduction. A nonhomogeneous structure is furthermore supported by photon correlation studies of the structural relaxation in PPO-$NaCF_3SO_3$ complexes,[37,38] dielectric spectroscopy data on PPO-$LiClO_4$,[39] and positron annihilation lifetime spectroscopy studies on PEO-$LiClO_4$.[40] On the other hand, small angle neutron scattering (SANS) studies of PPO-$LiClO_4$ (Ref. 26) and PEO-LiI (Ref. 41) show no indications of structural heterogeneities, and studies of PPO-$LiClO_4$ using neutron spin echo experiments[42] show results which are compatible with a structure with a marked nonhomogeneous distribution of ions only if it occurs on small length scales. Thus, there has been no direct observation of the suggested structure of microscopic salt-rich and salt-depleted domains, and the length scale of the domains is not identified.

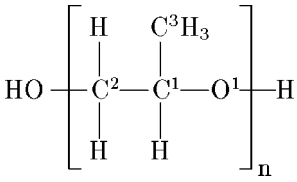

FIG. 1. The chemical structure formula of PPO. The superscripts number some atoms for later calculation of partial correlations.

Although the direct information in diffraction data is limited, much more can be extracted than the peaks in the pair distribution function. This concerns, in particular, the intermediate range order, which was discussed only qualitatively in the previous neutron diffraction studies. One way to extract quantitative information out of diffraction data is by the use of the RMC method. The method produces three-dimensional atomistic structural models based on experimental structure factors and any known constraints on the structure, e.g., on certain bond lengths or coordination numbers.

In the present work we analyze x-ray and neutron diffraction data of PPO-$LiClO_4$ using RMC simulations to determine the changes to the polymer host due to the solvated salt. A structural model suggested in our previous publications[23,25,26] is revised and refined. We investigate how the ions coordinate to the polymer chains, and the interionic correlations. The suggested heterogeneities of salt-rich and salt-depleted domains[35,36] are scrutinized. For purposes of comparison the study also includes results from an RMC simulation of pure PPO.[27]

II. EXPERIMENT

A. Sample preparation

Hydrogenous PPO of average molecular weight $M_w \approx 4000$ was purchased from Polysciences, Inc. Deuterated PPO was purchased from Polymer Source Inc. Both polymers were atactic with hydroxy end groups. The repeat unit of PPO is shown in Fig. 1. In the following, we use PPO_H and PPO_D to denote hydrogenous and deuterated PPO with specifications as above.

The molecular weight of the deuterated polymer was stated by the supplier to be $M_w=4300$, but subsequent characterization by gel-permeation chromatography and MALDI-TOF mass spectroscopy supports a significantly lower value, $M_w \approx 2000$.[43,44] NMR investigations of the deuterated polymer indicated that the methyl groups were fully deuterated and that $\approx 86\%$ of the hydrogen atoms attached to the polymer backbone were deuterated.[43] The neutron scattering cross section indicates that $\approx 90\%$ of the total number of hydrogens were deuterated.

Light-weight impurities were removed from the polymer samples by freeze drying on a vacuum line using more than eight cycles over a 96 h period. The polymer samples were thereafter kept in an argon atmosphere with a humidity <0.5 ppm until put into flat aluminum containers designed for neutron scattering. The sample space of the containers was 1 mm thick between 1 mm thick walls and was sealed with a gasket of indium wire.

In the preparation of the PPO-$LiClO_4$ samples, freeze-dried PPO was mixed with the $LiClO_4$ salt, which had been vacuum dried at 120 °C for several days, to obtain samples with molar ratios of ether oxygens per lithium atom 5:1 and 16:1. We will in the following use the notation PPO-$LiClO_4$ O:Li to refer to a polymer electrolyte with a specific lithium concentration. The salt was dissolved in the polymer under stirring at elevated temperature (~ 50 °C) using minute amounts of acetonitrile as intermediary solvent. The solution was placed in a vacuum furnace at 60 °C for more than eight weeks to let the acetonitrile evaporate. Thereafter the sample was transferred in dry argon atmosphere to the aluminum container designed for the scattering experiment as described above. There were no signs of any residual acetonitrile in the final samples when characterized by Raman spectroscopy.

B. Neutron diffraction experiments

The quantities measured in neutron diffraction experiments and their relation to the static structure factor $S(Q)$ and the radial distribution function $g(r)$, which are used to describe the structure in the present work, have been described previously.[27] A thorough treatment of the theory and applications of neutron diffraction can be found in Squires.[45]

In the different diffraction experiments of the present study the partial structure factors $S_{ij}(Q)$, which describe correlations between atoms of types i and j, have different weights in the total structure factors. More precisely, the experimental structure factor is given by

$$S(Q)=\frac{\Sigma_{i,j}c_i c_j b_i b_j[S_{ij}(Q)-1]}{\Sigma_i c_i b_i^2}+1, \tag{1}$$

following the Faber-Ziman formalism.[46] Here, c_i denotes the concentration and b_i the coherent scattering length for an element i.

Neutron scattering investigations of the static structure factor $S(Q)$ were performed on the low angle time-of-flight diffractometer SANDALS at ISIS, Rutherford-Appleton Laboratory, UK. SANDALS is specially designed for structural investigations of amorphous and liquid materials containing light atoms, such as hydrogen. For this purpose the detectors are placed at low angles to minimize inelastic scattering, which is otherwise a serious problem for such samples. Despite working at small angles, the time-of-flight method at a pulsed neutron source allows for measurements up to high momentum transfers (~ 30 Å^{-1}) with good statistics. For the present hydrogen rich polymers the inelastic scattering causes an almost divergent rise at low Q which, with the method used, cannot be perfectly corrected for. This makes the data less reliable for a momentum transfer $Q \lesssim 1$ Å^{-1}. Normalization of the data to a vanadium standard and corrections for absorption and multiple scattering were performed using the ATLAS program suite.[47,48] SANDALS was used to investigate deuterated PPO, PPO-$LiClO_4$ of concentrations O:Li$\approx$16:1 and 5:1, hydrogenous PPO, and PPO-$LiClO_4$ of concentration O:Li$\approx$16:1. All measurements were carried out at room temperature.

From the experimental structure factors of the different detector groups, $S(Q)$ and $g(r)$ were calculated using the inverse Monte Carlo method MCGR.[49] By constraining $g(r)$ to be zero up to the smallest interatomic distance, systematic errors in the experimental $S(Q)$ can be removed in the calculated $S(Q)$. MCGR furthermore includes an option to subtract a second-order polynomial from every detector group of experimental data, which can be used as an inelasticity correction. By this option, MCGR can be used to extract the static structure factor from the scattering data of hydrogenous materials despite the large incoherent inelastic contribution.

C. X-ray diffraction experiments

The main parts of the formalism for neutron scattering, including Eq. (1), can also be applied to x-ray diffraction. The scattering lengths then have to be replaced by the Q-dependent atomic form factors $f_i(Q)$ as described in a previous paper.[27] The form factors are at low Q values roughly proportional to the number of electrons in the atoms, although the detailed shape varies between atoms. A thorough treatment of the theory and applications of x-ray diffraction can be found in Warren.[50]

The x-ray diffraction experiments were performed on hydrogenous PPO and PPO-$LiClO_4$ of concentrations O:Li $=16:1$ and 5:1 using Station 9.1,[51] a high-precision powder diffractometer at the Synchrotron Radiation Source (SRS) situated at Daresbury Laboratory, UK. All measurements were carried out at room temperature. The measurements were made in transmission geometry for $2° < 2\theta < 80°$ using an x-ray wavelength of 0.689 Å. The data were experimentally corrected for inelastic Compton scattering[52] using the Warren-Mavel method[50] (Zr K edge), as developed for use on Station 9.1.[53] The data was furthermore corrected for scattering from the container, absorption, and polarization, and divided by the sum of the squared atomic form factors. Multiple scattering was assumed to be negligible.

III. REVERSE MONTE CARLO SIMULATIONS

The reverse Monte Carlo (RMC) simulation technique is a method that uses experimentally determined static structure factors and/or radial distribution functions of a disordered material to produce a computer model of its structure, which is in quantitative agreement with available structural data and the density. RMC uses a standard Metropolis Monte Carlo algorithm[54] to move particles within a simulation box with periodic boundary conditions. However, instead of minimizing the energy, the squared difference between the experimental structure factor and the structure factor of the configuration of particles in the box is minimized.[55,56] Thus, the RMC method does not require interatomic potentials, but instead accurate structural data, as input. Data from different

TABLE I. Constraints for distances (in Å) between atom types (as specified in Fig. 1) in the simulation. The oxygen atoms in the perchlorate ions are denoted by O^2. In the cases where only one value is given for a certain atom-atom distance, this value denotes the closest distance allowed. The constraints were based on interatomic distances found in literature data on molten polyethylene (Refs. 74 and 75), crystalline PPO (Ref. 76), amorphous poly(methyl methacrylate) (Ref. 59), crystalline $LiClO_4$ (Ref. 63), and PEO-$LiCF_3SO_3$ (Ref. 77).

Atoms	C^1	C^2	O^1	C^3	H	Li	Cl	O^2
C^1	2.5	1.4–1.75	1.3–1.65	2.1	1.0–1.25	1.5	1.5	1.5
C^2		2.5	1.3–1.65	1.4–1.76	1.0–1.25	1.5	1.5	1.5
O^1			2.5	2.1	1.6	1.5	1.5	1.5
C^3				2.5	1.0–1.25	1.5	1.5	1.5
H					1.6	1.0	1.0	1.0
Li						2.0	2.0	1.5
Cl							2.0	1.3–1.6
O^2								2.1

sources (neutron, x-ray, extended x-ray-absorption fine structure) may be simultaneously fitted. In RMC simulations of molecules with complex structure, e.g., polymers, initial configurations with the correct intramolecular structure are generally used, and the molecular structures are maintained throughout the simulations by the use of bond length and connectivity constraints. The conclusions that can be drawn from the RMC structures concerning properties that strongly depend on the directional character of chemical bonds, e.g., polymer conformations, are limited, since diffraction data provide only indirect information on such properties. Intermolecular forces, on the other hand, are mainly nondirectional, and considerable insights can be gained from the RMC structures on structural properties governed by these forces. In the present work, the RMC technique has been applied to create a structural model of pure PPO, PPO-$LiClO_4$ 16:1, and PPO-$LiClO_4$ 5:1 from the neutron and x-ray diffraction data.

A. Simulation procedure

To simulate the intermediate range structural order, the configuration has to be large enough so that the corresponding box size does not influence the simulation. An estimate of the minimum number of atoms N required is given by $N=\rho(2d)^3$, where ρ is the number density and d is the length scale of the intermediate range order. For a typical amorphous material, $N=5000-10\,000$. The configurations of the present study contained a single PPO chain of 1000 repeat units (10 000 atoms) and in case of the two polymer-salt complexes, 62 and 200 ions (Li^+ and ClO_4^-) were added to correspond to the ratios O:Li=16:1 and 5:1. Periodic boundary conditions were used in cubic boxes and the box length was given the value 45.84 Å for pure PPO, 46.38 Å for PPO-$LiClO_4$ 16:1, and 47.15 Å for PPO-$LiClO_4$ 5:1, which corresponds to the experimentally measured densities.[33]

The initial configuration of the polymer chain was built using a random walk with all nearest C–C and C–O distances set to 1.5 and 1.4 Å and all the C–C–O and C–O–C bond angles to 109.5° corresponding to ideal tetrahedral angles, and 115° since the C–O–C bonds are usually found to be slightly larger.[57–59] Thereafter, the constraints on the bond angles were released, and methyl groups and hydrogen atoms were added to the backbone creating an atactic PPO chain. To maintain physically realistic configurations, in the sense that there is no overlap of atoms and the atoms are correctly connected to form chains of proper repeat units, the RMC simulation was run with certain constraints applied. The constraints were of two kinds: specified atom-atom distance intervals and fixed neighbors. Table I shows the distances between different atom types allowed by the constraints. The fixed neighbors constraint was applied to ensure that the atoms were linked together in a proper polymer chain, i.e., that no covalent bonds were broken. The details and validity of the initial configuration of the pure polymer have been discussed in previous publications.[27,60]

To construct initial structures for the RMC simulations of PPO-$LiClO_4$, the structure of the pure PPO resulting from the RMC simulation of the pure polymer was used as the polymer host matrix. The box lengths were first scaled to correspond to the correct densities and the salt was added by randomly placing particles corresponding to Li^+ ions, and Cl and O atoms, the latter constrained to form ClO_4^- ions. The salt atoms were then moved (while keeping the polymer atoms in fixed positions) until the specified constraints on the interatomic distances were fulfilled. It is interesting to note that no rearrangements of the atoms in the polymer host were needed to fulfill these constraints, indicating a substantial free volume in the host, enough to accommodate the salt.

As experimental data in the RMC simulations of pure PPO and the polymer-salt complexes, structure factors obtained using neutron and x-ray diffraction on hydrogenous samples (no neutron data for PPO_H-$LiClO_4$ 5:1), and structure factors and radial distribution functions (the structural information is differently weighted in the two) obtained by neutron diffraction on deuterated samples were used. To account for the incomplete deuteration of the PPO_D samples in the simulation, an average scattering length $b=5.65$ fm was used for hydrogen atoms. This is however an approximation since the hydrogen isotopes are not randomly distributed (atoms in the methyl groups were fully deuterated while those in the backbone were not) which may introduce systematic errors in the RMC configurations. However, since only 6% of the total number of atoms are ^1H, the errors will be relatively small and mainly concern local correlations within the polymer chains, which are not the focus of the present study.

The simulations were run until no further reductions in the difference to the experimental data were obtained. The

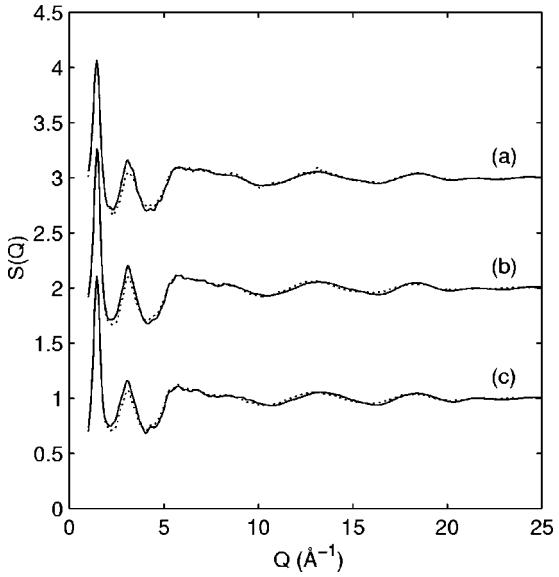

FIG. 2. Static structure factors $S(Q)$ of PPO (a), PPO-$LiClO_4$ 16:1 (b), and PPO-$LiClO_4$ 5:1 (c) as obtained from neutron diffraction experiments at room temperature on deuterated samples (solid lines) together with the corresponding $S(Q)$ from the RMC simulations (dotted). The structure factors have been normalized according to the formalism described in Ref. 27 and curves have been shifted vertically by steps of unity for clarity.

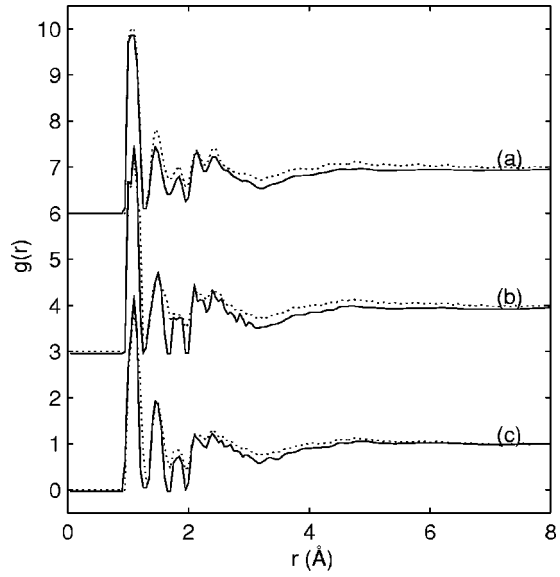

FIG. 3. Radial distribution function factors $g(r)$ of PPO_D (a), PPO_D-$LiClO_4$ 16:1 (b), and PPO_D-$LiClO_4$ 5:1 (c) as obtained by using the MCGR method on the static structure factors in Fig. 2 from neutron experiments (solid lines) and the corresponding $g(r)$ from the RMC simulations (dotted). The curves have been shifted vertically by steps of 3 for clarity.

average distance each atom had moved from its initial position was 2.1 Å for the pure polymer. This should be sufficient to effectively recreate the short and intermediate range order, but the long range chain behavior, such as the radius of gyration, remains controlled by the initial structure. In case of the polymer-salt complexes, the RMC structure of pure PPO was used as initial configuration for the polymer, which significantly reduces the modifications needed.

IV. RESULTS

In Fig. 2 we show the static structure factors $S(Q)$ as obtained from neutron diffraction experiments on PPO_D, PPO_D-$LiClO_4$ 16:1, and PPO_D-$LiClO_4$ 5:1. The figure also shows the corresponding static structure factors $S(Q)$ produced by the RMC simulations and, except for the Q range around the second peak in $S(Q)$ ($\sim 2.2-4.0$ Å^{-1}), the agreement with experimental data is seen to be excellent. The discrepancies around the second peak in $S(Q)$ may be attributed to residuals from subtraction of Bragg peaks from the aluminum sample container, which occur in this region.

Figure 3 shows the radial distribution functions $g(r)$ obtained from the experimental static structure factors $S(Q)$ in Fig. 2 using the inverse method MCGR.[49,61] For comparison, the corresponding radial distribution functions obtained from the RMC simulations are also shown. The well-defined peaks in the range $r<3$ Å can be attributed mainly to the short range order of the repeat units in the polymer chains and the perchlorate ions. The peaks in $g(r)$ arising from the repeat units may be assigned to interatomic correlations as follows: 1.1 Å to C–H, 1.5 Å to C–C and C–O, 1.8 Å to H–H, 2.1 Å to C–(C)–H,[62] C–(O)–H, O–(C)–H. For a more detailed discussion of the chemical short range order of the polymer chain, see our previous publication.[27] A close inspection of the peaks at 1.5 Å in Fig. 3 reveals an increasing peak area with increasing salt concentration. This may be attributed to the correlations between O^2 and Cl atoms in the ClO_4^- ion, which are separated roughly by 1.5 Å.[63] The systematic discrepancies between the $g(r)$ obtained from MCGR and those obtained from the RMC simulations in the region $2.5<r<7$ Å are caused by artificial peaks in $S(Q)$ in the range $Q=0.05-0.15$ Å^{-1}, which are produced in the MCGR procedure. These peaks are outside the data range used for the RMC simulation and do not affect the results.

Figure 4 shows the static structure factors $S(Q)$ as obtained from x-ray diffraction experiments on PPO_H, PPO_H-$LiClO_4$ 16:1, and PPO_H-$LiClO_4$ 5:1. The figure also shows the corresponding static structure factors $S(Q)$ produced by the RMC simulations and the agreement with experimental data is seen to be good. The discrepancies may be ascribed to systematic errors in the data, such as remnants of Compton scattering, absorption, or scattering from the container.

The static structure factors $S(Q)$ as obtained from neutron diffraction experiments on PPO_H and PPO_H-$LiClO_4$ 16:1 are shown in Fig. 5. Due to difficulties in correcting quantitatively for the inelastic scattering effects in the low Q range of $S(Q)$ for hydrogenous samples, we use only the range $Q>3$ Å^{-1} in the RMC simulations. The agreement between the static structure factors $S(Q)$ produced by the RMC simulations and the corresponding experimental data is fair. The discrepancies may, partly, be ascribed to systematic errors from inelastic scattering effects in the data. Small discrepancies will also arise from the quantum mechanical effects for the nuclear motion, which are different for H and D atoms. In the present case, these effects will result in slightly broader peaks in $g(r)$, and correspondingly, a stronger attenuation of oscillations in $S(Q)$ for correlations involving H atoms compared to D atoms.[64] We do therefore not expect

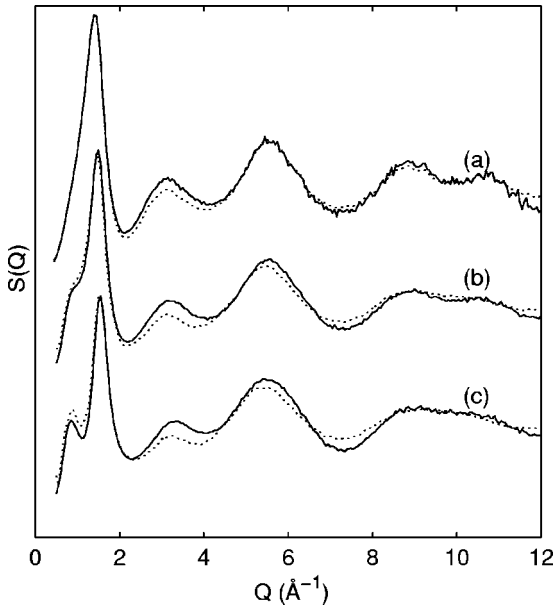

FIG. 4. Static structure factors $S(Q)$ of PPO_H (a), PPO_H-$LiClO_4$ 16:1 (b), and PPO_H-$LiClO_4$ 5:1 (c) as obtained from room temperature x-ray diffraction experiments (solid lines) together with the corresponding $S(Q)$ from the RMC simulations (dotted). The structure factors have an arbitrary normalization and curves have been shifted vertically for clarity.

data from deuterated and hydrogenous samples to be fully compatible.

In the results from the different experiments presented in Figs. 2–5 the partial structure factors $S_{ij}(Q)$, which describe correlations between atoms of types i and j, have different weights in the total experimental structure factors in accordance with Eq. (1). Table II summarizes the weights of the partial structure factors $S_{ij}(Q)$ with major contributions to the total $S(Q)$ in the different experiments. It is seen that the correlations between atoms in the polymer host by far dominates in the neutron scattering experiments on samples containing PPO_D. Since the curves in Fig. 2 are similar to a first approximation, this indicates that the structure of the polymer host is not fundamentally changed by the solvation of salt. The correlations between the polymer chains and the perchlorate ions are, as demonstrated in Table II, most pronounced in the $S(Q)$ from x-ray and neutron diffraction experiments on PPO_H-containing samples. The correlations between perchlorate ions also contribute significantly to $S(Q)$ in these experiments. In none of the experiments, however, do the correlations involving lithium have significant weight.

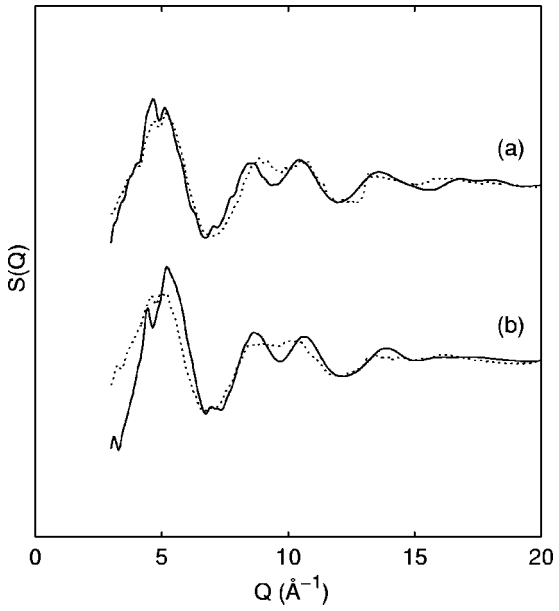

FIG. 5. Static structure factors $S(Q)$ of PPO_H (a) and PPO_H-$LiClO_4$ 16:1 (b) as obtained from neutron diffraction experiments at room temperature (solid lines) together with the corresponding $S(Q)$ from the RMC simulations (dotted). The structure factors have an arbitrary normalization and curves have been shifted vertically for clarity.

TABLE II. Weighting factors (normalized scattering coefficients) for the different correlations involving the polymer and/or ClO_4^- ions in x-ray (XD) and neutron (ND) diffraction experiments of hydrogenous (H) and deuterated (D) PPO-$LiClO_4$ of concentration O:Li=16:1. The values for the x-ray experiment are only approximate for $Q \neq 0$.

Correlation	D (ND)	H (ND)	H (XD)
PPO-PPO	0.944	0.398	0.839
ClO_4^--PPO	0.058	0.494	0.143
ClO_4^--ClO_4^-	0.001	0.153	0.006

The simultaneous agreement between the experimental structure factors and those produced in the RMC simulations (see Figs. 2–5) indicates that the structures produced in the RMC simulations contain the principal features of the real structures. Since the weight of the correlations involving lithium is low, we do not expect to reproduce the local order of the lithium ions with any significant accuracy. We therefore refrain from investigating the correlations involving Li ions and focus on the polymer matrix and the more strongly scattering anions.

V. ANALYSIS AND DISCUSSION

To investigate the interplay between the solvated salt and the polymer host matrix we compare the structures of PPO, PPO-$LiClO_4$ 16:1, and PPO-$LiClO_4$ 5:1 produced in the RMC simulations. We first focus on the structure of the polymer matrix and the changes to it induced by the salt. We then study the correlations between the polymer chains and the anions and, finally, we turn to the interanionic correlations. The structural features are analyzed and discussed in terms of partial and full static structure factors and radial distribution functions. When sums of partial structure factors are presented, weights according to the scattering lengths in deuterated samples are used.

A. The polymer matrix

Due to the chain topology of the molecules in the polymer host, it is instructive to separate the correlations between atoms belonging to the same chain (intrachain) from the correlations between atoms belonging to different chains (interchain). More precisely, we may distinguish correlations between atoms belonging to the same segment, i.e., atoms in a sequence of connected repeat units, from correlations between atoms belonging to segments separated by a sequence

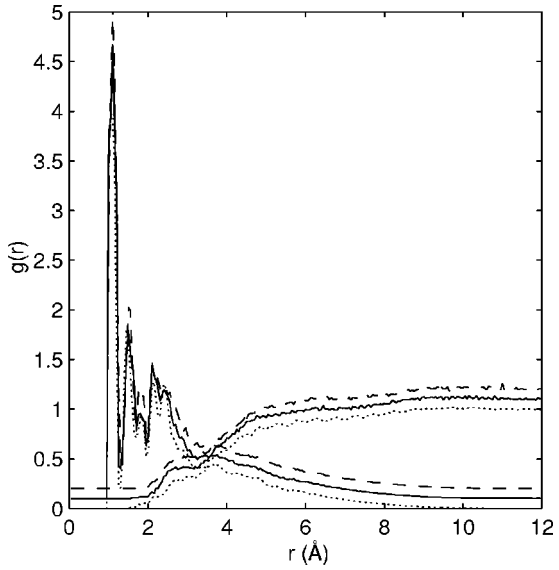

FIG. 6. Interchain and intrachain radial distribution functions $g^{\text{intra}}(r)$ and $g^{\text{inter}}(r)$ for PPO (dotted), PPO-$LiClO_4$ 16:1 (solid), and PPO-$LiClO_4$ 5:1 (dashed) as obtained from RMC simulations. The curves for the latter two have for clarity been shifted vertically by 0.1 and 0.2, respectively. At low r values, $g^{\text{intra}}(r)$ dominates whereas $g^{\text{inter}}(r)$ dominates at large r values.

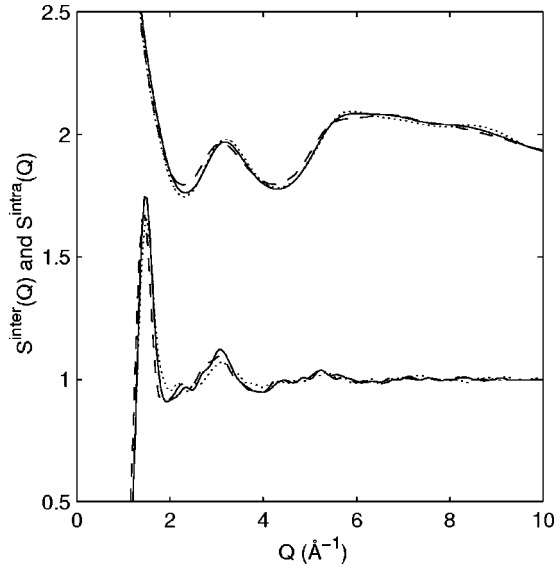

FIG. 7. Interchain and intrachain static structure factors $S^{\text{intra}}(Q)$ and $S^{\text{inter}}(Q)$ for PPO (dotted), PPO-$LiClO_4$ 16:1 (solid), and PPO-$LiClO_4$ 5:1 (dashed) as obtained from RMC simulations. $S^{\text{intra}}(Q)$ have been shifted vertically by 1.0 for clarity.

of several connected repeat units or physically different chains. For the neutron weighted radial distribution function $g(r)$ the separation between intrachain and interchain correlations can be expressed as

$$g^{\text{intra}}(r)=\sum_{i,j:|i-j|\leqslant s}^{N}\sum_{k,l}\frac{n_{kl}(r)b_k b_l}{4\pi r^2\Delta r\rho},$$

$$g^{\text{inter}}(r)=\sum_{i,j:|i-j|>s}^{N}\sum_{k,l}\frac{n_{kl}(r)b_k b_l}{4\pi r^2\Delta r\rho}, \tag{2}$$

where the summation indices i and j run over all repeat units 1,...,N numbered in sequence. The parameter s determines how far in sequence a repeat unit should be considered to contribute to intrachain or interchain correlations and was in the present study set to 2. (Changing the parameter s to 1 or 3 produces very small changes in the calculated correlation functions.) The indices k and l run over the atoms in repeat units i and j, respectively, and r is the distance between these atoms. $n_{kl}(r)$ denotes the number of atoms found between r and $r+\Delta r$, and ρ is the number density of the polymer.

Figure 6 presents $g^{\text{intra}}(r)$ and $g^{\text{inter}}(r)$ of deuterated PPO, PPO-$LiClO_4$ 16:1, and PPO-$LiClO_4$ 5:1 calculated from the structures produced in the RMC simulations. The curves have been normalized so that $g(r)=g^{\text{intra}}+g^{\text{inter}}\rightarrow 1$ as $r\rightarrow\infty$. Below $r\approx 3$ Å only minor differences between the $g(r)$ for the different samples are observed, thus demonstrating that the short range order of the polymer structure is largely unaffected by the salt solvation, as is also expected. Also at larger r values the differences appear small, but weak oscillations due to the intermediate range order are present, see inset of Fig. 8.

The intermediate range order is better investigated in the low Q region of $S^{\text{intra}}(Q)$ and $S^{\text{inter}}(Q)$, the Fourier transforms of $g^{\text{intra}}(r)$ and $g^{\text{inter}}(r)$, which are presented in Fig. 7. For comparison we show in the inset of Fig. 8 the oscillations in $g^{\text{inter}}(r)$ due to the intermediate range order; indeed, more marked features are seen in Fig. 7. The function $S^{\text{intra}}(Q)$ can be regarded as the molecular form factor where the molecule in this case is a sequence of repeat units, and as all form factors, $S^{\text{intra}}(Q)$ increases at small Q. Comparing $S^{\text{inter}}(Q)$ of PPO, PPO-$LiClO_4$ 16:1, and PPO-$LiClO_4$ 5:1, significant differences are seen in the first (sharp) diffraction peak (FSDP) around 1.5 Å^{-1}. Since the main part of this peak is reproduced in $S^{\text{inter}}(Q)$ it is evident that the peak originates from interchain correlations.[27,65] We observe that also in the region of the second peak of $S^{\text{inter}}(Q)$, that is, for $2\lesssim Q\lesssim 4$ Å^{-1}, the curves are dissimilar. There are also notable differences between $S^{\text{intra}}(Q)$ for $1.8\lesssim Q\lesssim 3$ Å^{-1}.

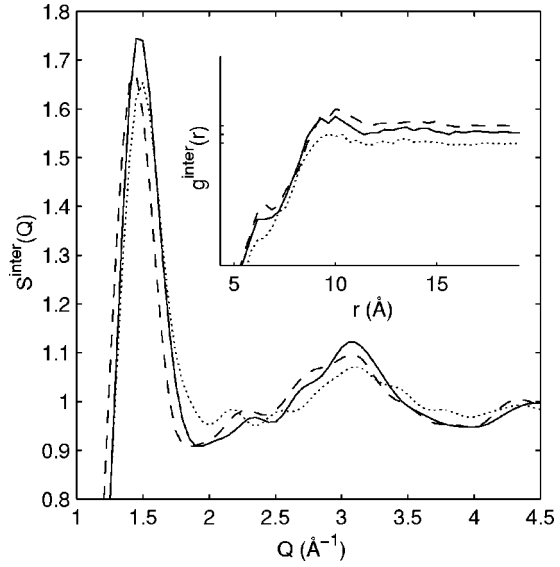

FIG. 8. $S^{\text{inter}}(Q)$ for PPO (dotted), PPO-$LiClO_4$ 16:1 (solid), and PPO-$LiClO_4$ 5:1 (dashed) as obtained from RMC simulations.

1. Interchain correlations

Let us now focus on the interchain correlations, and particularly on $S^{\text{inter}}(Q)$ and $g^{\text{inter}}(r)$ which are shown in Fig. 8. The position of the FSDP shifts slightly from $\approx 1.50\ \text{Å}^{-1}$ for PPO to $1.49\ \text{Å}^{-1}$ for PPO-$LiClO_4$ 16:1. For PPO-$LiClO_4$ 5:1 a larger shift to $1.43\ \text{Å}^{-1}$ is observed. The width of the FSDP does not change markedly with increasing salt concentration, although a wing in $S^{\text{inter}}(Q)$ for pure PPO at $\approx 1.75 \lesssim Q \lesssim 1.9\ \text{Å}^{-1}$ disappears as the salt concentration is increased to O:Li=16:1. The changes are significant, though small, since for PPO_D samples the scattering contrast of the polymer network is very high (see Table II), the systematic data errors due to imperfect data corrections are small and the reproduction of the FSDP in the RMC simulations, weighted according to PPO_D-$LiClO_4$ scattering lengths, is excellent.

The shift of the FSDP to lower Q values (corresponding to larger length scales) may be interpreted as the polymer matrix expanding as the salt is introduced. The shift of the FSDP does not follow the behavior of the density in a straightforward way. The density increases approximately linearly with increasing salt concentration,[33,66] corresponding to a nearly constant number density, $\rho \approx 0.104\ \text{Å}^{-3}$, and a number density for the polymer matrix, which decreases steadily from $0.104\ \text{Å}^{-3}$ for PPO to $0.101\ \text{Å}^{-3}$ for PPO-$LiClO_4$ 16:1 and to $0.095\ \text{Å}^{-3}$ for PPO-$LiClO_4$ 5:1.

The relatively small shift of the FSDP observed for PPO-$LiClO_4$ 16:1 signifies that the ions are introduced in a way which only marginally affects the characteristic interchain distances, the ions might, e.g., be found in the free volume already available in the pure polymer. As the salt concentration is increased to O:Li=5:1, the FSDP moves significantly to lower Q values, showing that the polymer matrix expands to host the ions. The expansion may be compared with that expected if the polymer matrix remains unstretched along the polymer chains and expands uniformly in the remaining two dimensions. Such an expansion corresponds to the position of the FSDP being proportional to the square root of the number density of the polymer matrix. The observed change in the position of the FSDP between PPO-$LiClO_4$ 16:1 and PPO-$LiClO_4$ 5:1 is even greater. A possible explanation for the large shift of the FSDP may be that the polymer-ion coordinations are qualitatively different at the two concentrations: in the 16:1 complex, the interchain structure of the pure polymer is largely retained and the ions have a limited effect on the characteristic interchain distance, whereas in the 5:1 complex, the ions have a more pronounced effect on the interchain distance and the chains are pushed apart. Such qualitatively different ion distributions were obtained in MD simulations of PEO-LiI;[19] whereas the ion distribution in PEO-LiI 15:1 is heterogeneous, it is much more homogeneous in PEO-LiI 5:1. Another factor that may also affect the interchain distance is that the fraction of cations cross-linking different chains decreases with salt concentration.[19,58]

In Fig. 8, the amplitude of the FSDP first increases with concentration from ≈ 1.67 for PPO to 1.75 for PPO-$LiClO_4$ 16:1 and then decreases to ≈ 1.67 for PPO-$LiClO_4$ 5:1. The same behavior is observed for the second peak in $S^{\text{inter}}(Q)$ for which the intensity increases as the pure polymer is doped to a concentration O:Li=16:1, and thereafter decreases as the concentration is increased to O:Li=5:1. Since the number of repeat units has not changed, these observations suggest that there are differences in the amplitude and attenuation of density oscillations due to the packing of the polymer chains. The increased amplitudes of the FSDP and the second peak thereby signify an increased ordering of the polymer chains in PPO-$LiClO_4$ 16:1 compared to PPO. As the salt concentration is increased to O:Li=5:1 the oscillations are again more damped and the ordering of the polymer chains is therefore interpreted to decrease.[67] In view of the suggested heterogeneous structure of PPO-$LiClO_4$ 16:1 and provided the salt-depleted regions are similar in structure to pure PPO, this indicates that the increased ordering is due to rather well-defined structural arrangements within the salt-rich regions and that the characteristic interchain distance in the salt-rich regions is similar to that of the pure polymer.

In this context, it is interesting to compare the present findings with previous neutron diffraction results for amorphous PEO-salt complexes. In d-PEO-LiTFSI 7.5:1,[21] d-PEO-$LiClO_4$ 6.5:1,[22] and d-PEO-LiI 5:1,[17] the FSDP observed in neutron diffraction data appears at $Q=1.5\ \text{Å}^{-1}$, which is similar to the value for pure d-PEO, $Q=1.45\ \text{Å}^{-1}$, but the amplitudes were higher than in the pure polymer. This indicates a higher degree of ordering in the PEO-salt complexes as well. An increase of the characteristic interchain distance in the PEO-salt complexes cannot be directly inferred from the position of the FSDP in those diffraction data, but could be a likely outcome of an analysis according to the present study.

2. Intrachain correlations

Turning to the intrachain correlations, significant differences between samples with varying salt concentration can be observed in the first valley in $S^{\text{intra}}(Q)$, see Fig. 7. The intrachain property that can be expected to change the most is the conformation. A common description of the conformation is by the dihedral angles, which describe the correlation between four sequential atoms in the chain. The dihedral angles are strongly affected by the directional character of the bonds, and they are therefore likely to be poorly reproduced in the RMC simulations to which the input is based only on pair correlations. Figure 9 shows the distribution of dihedral angles φ for the atom sequence $O^1-C^1-C^2-O^1$ for PPO, PPO-$LiClO_4$ 16:1, and PPO-$LiClO_4$ 5:1. The distributions found in the RMC simulations are indeed very broad; they have *trans* peaks, but no clear *gauche* peaks. The dihedral angle distributions for the atom sequences $C^1-C^2-O^1-C^1$ and $C^2-O^1-C^1-C^2$ show basically the same characteristics and salt concentration dependencies. To obtain the fraction of dihedral angles in different states, we define the range $0° \leqslant \varphi < 120°$ as *gauche* states and $120° \leqslant \varphi < 180°$ as *trans* states. The resulting fraction of *gauche* conformations for PPO is $\approx 50\%$, and for the polymer salt complexes $\approx 55\%$. These figures can be compared with molecular dynamics simulations of PPO (Ref. 65) where *gauche* fractions of 61% for the O–C–C–O dihedrals and 35% for the C–C–O–C backbone dihedrals were found. The higher

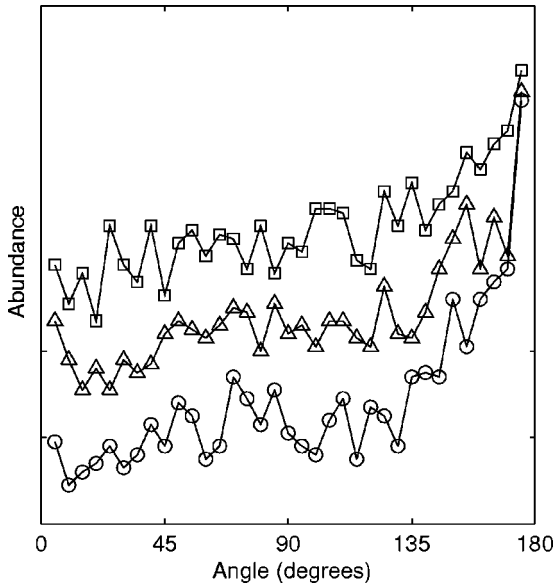

FIG. 9. The dihedral angle distributions for $O^1-C^1-C^2-O^1$ in PPO (rings), PPO-$LiClO_4$ 16:1 (triangles, shifted vertically to first tick), and PPO-$LiClO_4$ 5:1 (squares, shifted vertically to second tick).

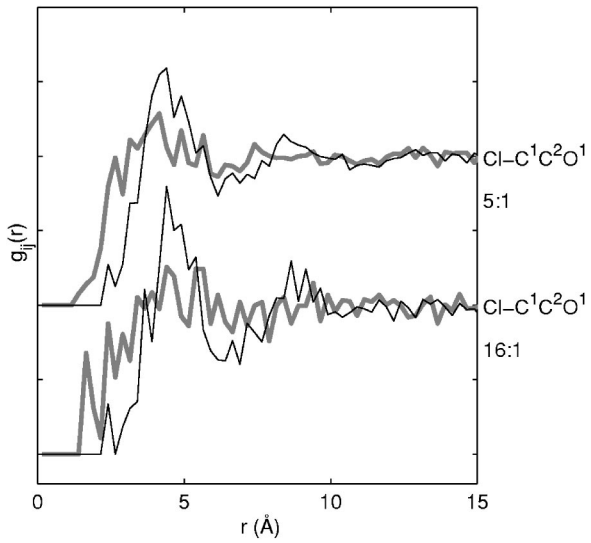

FIG. 10. The partial $g_{Cl-C^1C^2O^1}(r)$ for PPO-$LiClO_4$ 16:1 and PPO-$LiClO_4$ 5:1 from the RMC simulations (thin solid black lines) and the initial configuration for the RMC simulation (bold gray lines), i.e., from a hard-sphere Monte Carlo simulation. All curves are normalized to unity for large r values.

fractions of *gauche* conformations for the O–C–C–O dihedrals in the electrolytes is in accordance with MD simulations of PEO-LiI and tetraglyme-$LiCF_3SO_3$,[68,69] and spectroscopic investigations of PPO complexed with lithium salts.[70,71]

What can be learned from the dihedral angle distributions of the RMC structures? While they in comparison to other studies[65,69] fail to produce distinct *gauche* peaks, they correctly reproduce two important features: a *trans* peak and the increasing fraction of *gauche* states with increasing salt concentration. (The distribution is flat in the initial configuration based on a freely rotating polymer.) This indicates that what is mainly reproduced in the RMC structure is the local contour of the polymer chain; a *trans* peak is required to obtain a realistically stretched chain. The variation in the fraction of *gauche* states with salt concentration is also reflected in the polymer coil dimensions, as has been observed using SANS.[18]

B. Polymer-ion correlations

Having considered various aspects of interchain and intrachain structural correlations, we turn to the correlations between the ClO_4^- ions and the polymer chains. As mentioned above, we refrain from analyzing correlations involving Li ions since they contribute too weakly to the structure factors obtained by neutron and x-ray diffraction in the present case. The polymer-anion correlations may be investigated in $g_{ij}(r)$ where i denote Cl and j the atoms in the polymer repeat units. We focus on the correlations between the ions and the polymer backbone, i.e., C^1, C^2, and O^1, and use the notation $g_{Cl-C^1C^2O^1}(r)$ for the sum of the $g_{Cl-C^1}(r)$, $g_{Cl-C^2}(r)$, and $g_{Cl-O^1}(r)$ with weights according to their concentrations and neutron scattering lengths. Figure 10 shows these correlations in terms of $g_{ij}(r)$ as obtained from the RMC simulations of PPO-$LiClO_4$ 16:1 and PPO-$LiClO_4$ 5:1, and for the corresponding initial configurations.

For PPO-$LiClO_4$ 16:1 we observe in $g_{Cl-C^1C^2O^1}(r)$ a pronounced but broad peak at $r \approx 4.5$ Å followed by a less pronounced peak at $r = 8-9$ Å. For PPO-$LiClO_4$ 5:1 peaks are seen at approximately the same positions, though the peaks are broader compared to the sample with lower salt concentration.[67] For the corresponding initial structures only faint and broadened peaks are seen in $g_{Cl-C^1C^2O^1}(r)$. This indicates a rather well-defined distance between the ClO_4^- ions and the polymer chain, which is not due to hard-sphere excluded-volume effects (which are accounted for in the initial structures). The observation may seem rather surprising since the anions, which have a distributed charge, are expected to interact only weakly with the polymer chains.[2] However, a likely explanation is that cations coordinated to ether oxygens also coordinate one or more anions. The increased correlation is thereby mediated via a cation. A weakly repelling interaction between the polymer chains and the anions may also cause an effectively stronger correlation since the anions are surrounded by polymer chains. In particular, the peak at $r \approx 4.5$ Å fits nicely with the structure predicted in MD simulations of PEO-LiI (Ref. 68) and PEO-NaI,[58] with a relatively planar crown-ether-like coordination of PEO around the cation, and the anion coordinated to the cation normal to that plane.

C. Interanionic correlations

Turning to the interanionic correlations, Table II shows that the ClO_4^--ClO_4^- correlations contribute a large part to the static structure factor only in the neutron diffraction experiments on hydrogenous samples. In the RMC simulation of PPO-$LiClO_4$ 16:1, the short range order interanionic correlations should be well reproduced based on $S(Q)$ from neutron scattering on PPO_H-$LiClO_4$ 16:1, though since only

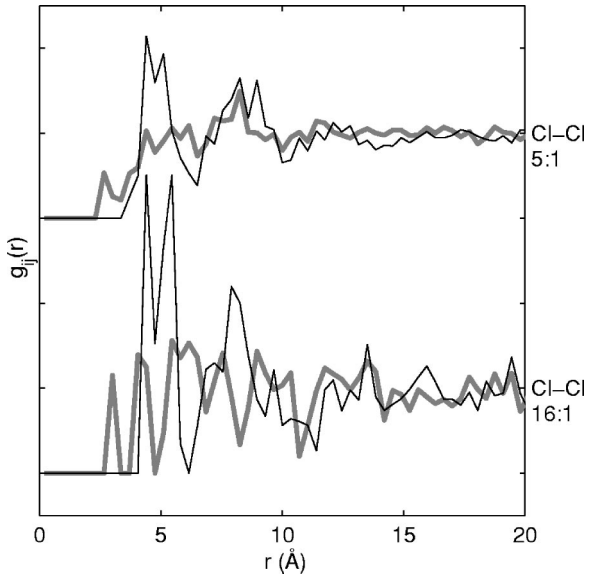

FIG. 11. The partial $g_{\mathrm{Cl-Cl}}(r)$ for PPO-$LiClO_4$ 16:1 and PPO-$LiClO_4$ 5:1 from the RMC simulations (thin solid black lines) and the initial configuration for the RMC simulation (bold gray lines). All curves are normalized to unity for large r values.

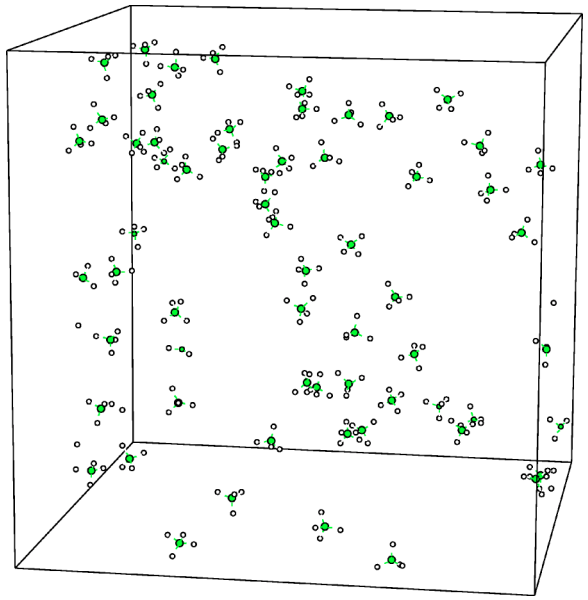

FIG. 12. Positions of ClO_4^- ions in the simulation box of the RMC simulation of PPO-$LiClO_4$ 16:1.

$S(Q>3)$ Å^{-1} was used as input to the simulations the long range order must be expected to be reproduced with less accuracy. However, indirect information on the long range interanionic correlations is incorporated in the simulations by the requirement that the interanionic long range order is consistent with the short range order, the polymer structure, and constraints on, e.g., the density and excluded volume of atoms. Indeed, the requirement of consistency is one of the great virtues using the RMC method to interpret diffraction data.

To investigate the ClO_4^--ClO_4^- correlations we study $g_{\mathrm{Cl-Cl}}(r)$ which describe the correlation between the centers of the anions. Figure 11 shows these correlation functions for PPO-$LiClO_4$ 16:1 and PPO-$LiClO_4$ 5:1. For comparison, also $g_{\mathrm{Cl-Cl}}(r)$ of the initial configurations for the RMC simulations are shown. As is seen in the figure, $g_{\mathrm{Cl-Cl}}(r)$ for the configurations obtained in the RMC simulations for PPO-$LiClO_4$ 16:1 and PPO-$LiClO_4$ 5:1 exhibit clear correlation peaks at $r \approx 5$ Å and at $r \approx 8$ Å. The similarities between the $g_{\mathrm{Cl-Cl}}(r)$ for the two salt concentrations indicate, since no neutron diffraction data on hydrogenous PPO-$LiClO_4$ 5:1 were used, that information about the anion positions is contained in the structure of the polymer and in the polymer-anion coordinations.

The corresponding $g_{\mathrm{Cl-Cl}}(r)$ for the initial structures show only a gradual increase to the average density, confirming an initially homogeneous distribution of the ClO_4^- ions. We may interpret the first correlation peak at $r \approx 5$ Å, at least in part, as being due to the nearest Cl–Cl distance in ionic triplets or clusters, containing both anions and cations. It is interesting to note that MD simulations of PEO-LiI and PEO-NaI (Refs. 58 and 68) predict almost planar crown-ether-like coordination of the polymer ether oxygens around the cations where the anions may coordinate to the cations in rather well-defined configurations which would yield distinct interanionic correlations. Similar configurations in PPO-$LiClO_4$ may be the origin of the peaks in $g_{\mathrm{Cl-Cl}}(r)$.

Figures 12 and 13 show the positions of the ClO_4^- ions in the final and initial configurations, respectively, from the RMC simulation of PPO-$LiClO_4$ 16:1. Large concentration fluctuations of anions in the polymer host are seen in Fig. 12. Inspection of Fig. 12 reveals two clearly anion free voids with diameters which we estimate to roughly 10 Å. The (long range order) anion concentration fluctuations may be seen as a consequence of a required short range order, demonstrated by the peaks in $g_{\mathrm{Cl-Cl}}(r)$. Assuming that the fluctuations of charge cannot be large, the fluctuations in the anion concentration may be considered to follow the concen-

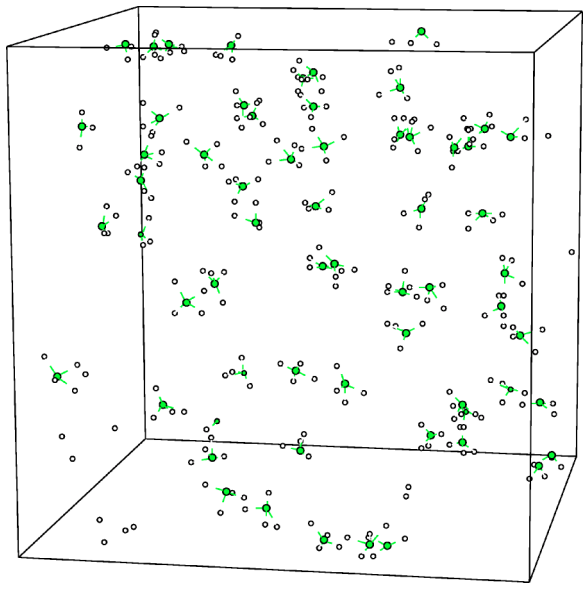

FIG. 13. Positions of ClO_4^- ions in the simulation box for the initial configuration for RMC simulation of PPO-$LiClO_4$ 16:1.

tration fluctuations of cations, and a required short range anion order may thus be interpreted as a preferred local salt concentration.

Since the RMC method generally produces the most disordered structure that is consistent with the input data, the fluctuations in the RMC structure strongly support the presence of salt-rich and salt-depleted regions in PPO-$LiClO_4$ 16:1 which has been suggested based on calorimetric studies.[35,36] The length scale of the concentration fluctuations must however be regarded as a coarse estimate due to the limited accuracy on long range interanionic correlations. The calorimetric measurements indicate that the PPO-$LiClO_4$ complexes are characterized by a structure of salt-rich and salt-depleted regions, which have different glass transition temperatures, and that for high salt concentrations, O:Li $<10:1$, only a salt-rich structure is present.[35,36] Photon correlation studies of PPO complexed with salts suggest similar structures.[37,38]

Results of recent investigations of the relaxation dynamics of the polymer host in PPO-$LiClO_4$ 16:1 using neutron spin echo experiments, which probe a length scale of ≈ 5 Å, are, however, incompatible with a structure consisting of microscopic salt-rich and salt-depleted domains of appreciably larger dimensions.[42,72] Nor did we find any indications in previous small angle neutron scattering (SANS) studies of PPO-$LiClO_4$ (Ref. 26) of heterogeneities on the length scale 20–500 Å. Similar results have also been found in SANS studies of deuterated PEO-LiI.[41]

For PPO-$LiClO_4$, an upper limit of the length scale of the heterogeneities must be of the order of 5000 Å by noting that the refraction index of the polymer salt complex is different from the pure polymer[33] and observing[36] that the complex is optically clear. Altogether, this indicates that the salt-rich and salt-depleted domains have to occur on a length scale less than 20 Å. To scrutinize these interpretations and determine the length scale of the domains we propose to investigate the length scale of 5–100 Å in a small angle (x-ray or neutron) scattering experiment. A possible explanation to the discrepancies between studies are that salt solvation and precipitation in some polyether salt complexes may be dependent on temperature and thermal history.[73]

VI. CONCLUSIONS

We present the first reverse Monte Carlo simulation study of an amorphous polymer electrolyte, PPO-$LiClO_4$, based on neutron and x-ray diffraction data. The simulations confirm, as suggested in our previous publications,[23,25,26] that the solvation of salt induces increased ordering of the polymer matrix. At variance with our previous interpretations of experimental data,[23,25,26] no contraction of the interchain distance is observed as the salt concentration increases. For PPO-$LiClO_4$ 16:1 we find that the interchain distance is approximately the same as in the pure polymer, although more well defined, which indicates that there is enough free volume in the pure polymer to host the ions. In view of the suggested heterogeneous structure of PPO-$LiClO_4$ 16:1, and provided the salt-depleted regions are similar in structure to pure PPO, this indicates that the increased ordering is due to rather well-defined structural arrangements within the salt-rich regions, and that the characteristic interchain distance in the salt-rich regions is similar to that of the pure polymer. For a higher salt concentration, O:Li$=5:1$, the polymer matrix must however expand to host the salt, which is reflected in a larger interchain distance. The polymer matrix in PPO-$LiClO_4$ 5:1 also exhibits a smaller degree of ordering compared to PPO-$LiClO_4$ 16:1. In comparison to other studies,[65,69] the dihedral angle distributions of the RMC structures are rather broad and do not exhibit distinct *gauche* peaks. They do, however, exhibit two important features: a *trans* peak and the increasing fraction of *gauche* states with increasing salt concentration.

The RMC simulations show that there are interanionic correlation distances of ≈ 5 Å, with a likely origin in ionic triplets or clusters involving cations, anions, and the ether oxygens of the polymer chains. The simulations for PPO-$LiClO_4$ 16:1 also indicate a spatially inhomogeneous ion distribution into salt-rich and salt-depleted domains, which when taking results in literature into account, should have a length scale of less than 20 Å. Since the RMC method generally produces the most disordered structure that is consistent with the input data this strongly supports the presence of a domain structure, on which there, in literature, has been no consensus.

The simulations demonstrate a rather strong correlation between the anions and the polymer chains which cannot be ascribed to an excluded volume effect. The anions are however expected to interact weakly with the polymer chains. We therefore propose that the effect is due to an arrangement where a cation is partially solvated by ether oxygens in a polymer chain and is also coordinated to an anion, thus introducing a significant correlation between the polymer chain and the anion. We note, however, that a weakly repelling interaction between the polymer chains and the anions may also cause an effectively stronger correlation since the anions are surrounded by polymer chains.

ACKNOWLEDGMENTS

The program was financially supported by the Swedish Research Council. J.S. is a Royal Swedish Academy of Sciences Research Fellow supported by a grant from the Knut and Alice Wallenberg Foundation.

[1] M. B. Armand, J. M. Chabagno, and M. J. Duclot, in *Extended Abstracts*, Second International Conference on Solid Electrolytes (The conference organisers, St. Andrews, Scotland, 1978).
[2] F. M. Gray, *Polymer Electrolytes, Fundamentals and Technological Applications* (The Royal Society of Chemistry, Cambridge, UK, 1997).
[3] V. A. Payne, M. C. Lonergan, M. Forsyth, M. A. Ratner, D. F. Shriver, S. W. de Leeuw, and J. W. Perram, Solid State Ionics **31**, 171 (1995).
[4] L. M. Torell and C. A. Angell, Br. Polym. J. **20**, 173 (1988).
[5] M. A. Ratner, in *Polymer Electrolyte Reviews*, edited by J. R. MacCallum and C. A. Vincent (Elsevier, London, 1987), Vol. 1, Chap. 7.
[6] L. M. Torell and S. Schantz, J. Non-Cryst. Solids **131**, 981 (1991).
[7] P. Lightfoot, M. A. Mehta, and P. G. Bruce, Science **262**, 883 (1993).
[8] P. Lightfoot, M. A. Mehta, and P. G. Bruce, J. Mater. Chem. **2**, 379 (1992).
[9] Y. Chatani and S. Okamura, Polymer **28**, 1815 (1987).
[10] Y. Chatani, Y. Fujii, T. Takayanagi, and A. Honma, Polymer **31**, 2238 (1990).
[11] C. D. Robitaille and D. Fauteaux, J. Electrochem. Soc. **133**, 315 (1986).
[12] G. S. MacGlashan, Y. G. Andreev, and P. G. Bruce, Nature (London) **398**, 792 (1999).

[13] I. Martin-Litas, Y. G. Andreev, and P. G. Bruce, Chem. Mater. **14**, 2166 (2002).
[14] C. P. Rhodes, M. Khan, and R. Frech, J. Phys. Chem. B **106**, 10330 (2002).
[15] Y. G. Andreev and P. G. Bruce, J. Phys.: Condens. Matter **13**, 8245 (2001).
[16] C. Berthier, W. Gorecki, M. Minier, M. B. Armand, J. M. Chabagno, and P. Rigaud, Solid State Ionics **11**, 91 (1983).
[17] J. D. Londono, B. K. Annis, A. Habenschuss, O. Borodin, G. D. Smith, J. Z. Turner, and A. K. Soper, Macromolecules **30**, 7151 (1997).
[18] B. K. Annis, M.-H. Kim, G. D. Wignall, O. Borodin, and G. D. Smith, Macromolecules **33**, 7544 (2000).
[19] O. Borodin and G. D. Smith, Macromolecules **31**, 8396 (1998).
[20] O. Borodin and G. D. Smith, Macromolecules **33**, 2273 (2000).
[21] G. Mao, M.-L. Saboungi, D. L. Price, M. B. Armand, and W. S. Howells, Phys. Rev. Lett. **84**, 5536 (2000).
[22] G. Mao, M.-L. Saboungi, D. L. Price, Y. S. Baydal, and H. E. Fischer, Europhys. Lett. **54**, 347 (2001).
[23] P. Carlsson, B. Mattsson, J. Swenson, L. Börjesson, L. M. Torell, R. L. McGreevy, and W. S. Howells, Electrochim. Acta **43**, 1545 (1998).
[24] P. Carlsson, J. Swenson, L. Börjesson, R. L. McGreevy, P. Jacobsson, L. M. Torell, and W. S. Howells, Electrochim. Acta **45**, 1449 (2000).
[25] P. Carlsson, J. Swenson, R. L. McGreevy, B. Gabrys, W. S. Howells, L. Börjesson, and L. M. Torell, Physica B **234-236**, 231 (1997).
[26] P. Carlsson, B. Mattsson, J. Swenson *et al.*, Solid State Ionics **115**, 139 (1998).
[27] P. Carlsson, J. Swenson, L. Börjesson, L. M. Torell, R. L. McGreevy, and W. S. Howells, J. Chem. Phys. **109**, 8719 (1998).
[28] See Special Issue on *Ion Conductivity in Polymers* L. M. Torell, P. Jacobsson, and G. Petersen, Polym. Adv. Technol. **4**, 152 (1993).
[29] J. R. MacCallum, A. S. Tomlin, and C. A. Vincent, Eur. Polym. J. **22**, 787 (1986).
[30] P. Fuinan, M. Xu, E. M. Eyring, and S. Petrucci, J. Phys. Chem. **97**, 3606 (1993).
[31] A. Bernson and J. Lindgren, Solid State Ionics **60**, 31 (1993).
[32] M. G. McLin and C. A. Angell, J. Phys. Chem. **95**, 9464 (1991).
[33] W. Wixwat, Y. Fu, and J. R. Stevens, Polymer **32**, 1181 (1991).
[34] J. R. Stevens and S. Schantz, Polym. Commun. **29**, 230 (1988).
[35] C. Vachon, M. Vasco, M. Perrier, and J. Prud'homme, Macromolecules **26**, 4023 (1993).
[36] C. Vachon, C. Labrèche, A. Vallée, S. Besner, M. Dumont, and J. Prud'homme, Macromolecules **28**, 5585 (1995).
[37] R. Bergman, L. Börjesson, G. Fytas, and L. M. Torell, J. Non-Cryst. Solids **172**, 830 (1994).
[38] R. Bergman, A. Brodin, D. Engberg, Q. Lu, C. A. Angell, and L. M. Torell, Electrochim. Acta **40**, 2049 (1995).
[39] T. Furukawa, Y. Mukasa, T. Suzuki, and K. Kano, J. Polym. Sci., Part B: Polym. Phys. **40**, 613 (2002).
[40] D. Bamford, A. Reiche, G. Dlubek, F. Alloin, J.-Y. Sanchez, and M. A. Alam, J. Chem. Phys. **118**, 9420 (2003).
[41] A. Triolo, F. Lo Celso, V. Arrighi *et al.*, Physica A **304**, 308 (2002).
[42] P. Carlsson, R. Zorn, D. Andersson, B. Farago, W. S. Howells, and L. Börjesson, J. Chem. Phys. **114**, 9645 (2001).
[43] J. Allgaier (private communication).
[44] J. Lausmaa, Chemistry and Materials Technology, Swedish National Testing and Research Institute Report No. 99k40908 (1999).
[45] G. L. Squires, *Introduction to the Theory of Thermal Neutron Scattering* (Cambridge University Press, Cambridge, 1978).
[46] T. E. Faber and J. M. Ziman, Philos. Mag. **11**, 153 (1965).
[47] J. Z. Turner, A. K Soper, W. S. Howells, and A. C. Hannon, *SANDALS Survival Guide* (Rutherford-Appleton Laboratory, UK, 1995).
[48] A. K. Soper, W. S. Howells, and A. C. Hannon, *ATLAS Analysis of Time-of-Flight Diffraction Data from Liquid and Amorphous Samples* (Rutherford-Appleton Laboratory, UK, 1989).
[49] M. A. Howe, R. L. McGreevy, and L. Pusztai, *MCGR* (Studsvik Neutron Research Laboratory, Nyköping, 1996).
[50] B. E. Warren, *X-ray Diffraction* (Addison-Wesley, Reading, MA 1969).
[51] G. Bushnell-Wye and R. J. Cernik, Rev. Sci. Instrum. **63**, 999 (1992).
[52] A. H. Compton, Phys. Rev. **21**, 483 (1923).
[53] G. Bushnell-Wye, J. Turner, J. L. Finney, D. W. Huxley, and J. C. Dore, Rev. Sci. Instrum. **63**, 1153 (1992).
[54] N. Metropolis, A. W. Rosenbluth, M. N. Rosenbluth, A. H. Teller, and E. Teller, J. Chem. Phys. **21**, 1087 (1953).
[55] R. L. McGreevy and L. Pusztai, Mol. Simul. **1**, 359 (1988).
[56] D. A. Keen and R. L. McGreevy, Nature (London) **344**, 423 (1990).
[57] Y. Takahashi and H. Tadokoro, Macromolecules **6**, 672 (1973).
[58] S. Neyertz and D. Brown, J. Chem. Phys. **104**, 3797 (1995).
[59] D. J. Ward and G. R. Mitchell, Phys. Scr. **T57**, 153 (1995).
[60] J. Swenson, P. Carlsson, L. Börjesson, L. M. Torell, R. L. McGreevy, and W. S. Howells, Comput. Theor. Polym. Sci. **10**, 465 (2000).
[61] L. Pusztai and R. L. McGreevy, Physica B **234**, 357 (1986).
[62] The atom in parenthesis denote the atom to which the correlated atoms are bonded.
[63] A. Sequira, I. Bernal, I. D. Brown, and R. Faggiari, Acta Crystallogr., Sect. B **31**, 1735 (1975).
[64] M. Slabanja and G. Wahnström, Chem. Phys. Lett. **342**, 593 (2001).
[65] P. Ahlström, O. Borodin, G. Wahnström, E. Wensink, P. Carlsson, and G. D. Smith, J. Chem. Phys. **112**, 10669 (2000).
[66] J. Moacanin and E. F. Cuddihy, J. Appl. Polym. Sci. **14**, 313 (1966).
[67] It might be argued that the reason for the less ordered RMC structure of PPO-$LiClO_4$ 5:1 is that the experimental input to that RMC simulation, in contrast to those of PPO and PPO-$LiClO_4$ 16:1, did not include a structure factor from neutron diffraction on a hydrogenous sample. However, since only the high-Q parts of the $S(Q)$ for the hydrogenous samples were used, this difference should only affect the short range order and not the intermediate range order.
[68] F. Müller-Plathe and W. F. van Gunsteren, J. Chem. Phys. **103**, 4745 (1995).
[69] J.-K. Hyun, H. Dong, C. P. Rhodes, R. Frech, and R. A. Wheeler, J. Phys. Chem. B **105**, 3329 (2001).
[70] S. Yoon, K. Ichikawa, W. J. MacKnight, and S. L. Hsu, Macromolecules **28**, 4278 (1995).
[71] H. Ericson, B. Mattsson, L. M. Torell, H. Rinne, and F. Sundholm, Electrochim. Acta **43**, 1401 (1998).
[72] Due to the short experimental length scale, the local dynamics of domains of appreciably larger size should be additive and result in a total relaxation function which is the superposition of the relaxation of the pure polymer and the (slower) relaxation in the salt-rich domains. The shape of the relaxation function is, however, found to be temperature independent within the investigated temperature range $T=260-334$ K, which is not compatible with such a relaxation function. Rather, the data indicate that the dynamics of the whole polymer matrix is affected by the salt solvation.
[73] M. Bégin, C. Vachon, C. Labrèche, B. Goulet, and J. Prud'homme, Macromolecules **31**, 96 (1998).
[74] B. Rosi-Schwartz and G. R Mitchell, Polymer **35**, 5398 (1994).
[75] B. Rosi-Schwartz and G. R Mitchell, Phys. Scr. **T57**, 161 (1995).
[76] E. Stanley and M. Litt, J. Polym. Sci. A **43**, 453 (1960).
[77] P. G. Bruce, Electrochim. Acta **40**, 2077 (1995).